第 30 卷第 6 期
2014 年 6 月

无 机 化 学 学 报
CHINESE JOURNAL OF INORGANIC CHEMISTRY

Vol.30 No.6
1395-1402

# 4-氯苯氧乙酸和 1,10-邻菲啰呤构筑的双核铽配合物的晶体结构，荧光和生物活性

徐 俊*,[1] 马德运[2] 覃 亮[2]

([1]暨南大学药学院，广州 510326)

([2]肇庆学院化学化工学院，肇庆 526061)

**摘要**：水热条件下采用 Tb $(NO_3)_3 \cdot 6$ $(H_2O)$,4-氯苯氧乙酸和 1,10-邻菲啰呤作为反应物合成出 1 个双核铽配合物 $[Tb_2(4\text{-Hcpoa})_5(phen)_2(NO_3)]$(**1**)(4-Hcpoa=4-氯苯氧乙酸，phen=1,10-邻菲啰呤)，并分别用元素分析、红外光谱、差热分析、X-射线粉末衍射和 X-射线单晶衍射等表征了该结构。晶体结构分析结果表明：2 个双齿和 2 个三齿 4-氯苯氧乙酸配体将 2 个铽金属离子连接成二聚体结构。荧光分析表明常温固态下配合物 **1** 发射绿色荧光，且在 544 nm 处的荧光寿命为 0.920 ms。以除草剂精喹禾灵为对照品，研究了配体 4-氯苯氧乙酸及其配合物 **1** 对甘蓝型油菜和钝芒稗的抑制作用。

**关键词**：铽配合物；水热合成；晶体结构；荧光性质；生物活性

**中图分类号**：O614.341 **文献标识码**：A **文章编号**：1001-4861(2014)06-1395-08

**DOI**：10.11862/CJIC.2014.215

# A Terbium Complex Constructed from 4-Chlorophenoxyacetate and 1,10-Phenanthroline with Luminescence and Biological Activity Studies

XU Jun*,[1] MA De-Yun[2] QIN Liang[2]

([1]*College of Medicine, Jinan University, Guangzhou* 510632, *China*)

([2]*School of Chemistry and Chemical Engineering, Zhaoqing University, Zhaoqing, Guangdong* 526061, *China*)

**Abstract**: A dinuclear terbium(Ⅲ) complex, $[Tb_2(4\text{-Hcpoa})_5(phen)_2(NO_3)]$ (**1**) (1, 4-Hcpoa=4-chlorophenoxyacetate, phen =1, 10-phenanthroline), has been hydrothermally synthesized and structurally characterized by elemental analysis, IR spectroscopy, TGA, powder X-ray diffraction and single crystal X-ray diffraction. Structural determination reveals that the $Tb^{3+}$ ions are bridged by two bidentate and two terdentate carboxylate groups to give a centrosymmetric dimer with Tb … Tb separations of 0.397 0 (2) nm. Solid-state **1** emits the intensely green photoluminescence with fluorescence lifetime of 0.920 ms (544 nm) at room temperature. The 4-Hcpoa ligand and complex **1** have been screened for their phytogrowth-inhibitory activities against *Brassica napus L.* and *Echinochloa crusgalli L.*, and the results are compared with the activity of quizalofop-*p*-ethyl. CCDC: 957432.

**Key words**: terbium(Ⅲ) complex; hydrothermal synthesis, crystal structure, luminescence; biological activity

In recent years, the design and synthesis of lanthanide complexes have attracted considerable attention in the areas of coordination chemistry, not only because of their intriguing variety of architectures and topologies, but also owing to their potential applications in luminescent materials, magnetic materials, catalysts, as luminescent probes, porous materials, biological chemistry, and so on[1-7].

收稿日期：2013-09-02。收修改稿日期：2014-01-23。

国家自然科学基金青年项目(81202461)中国博士后科学基金面上项目(2013M531906)资助。

*通讯联系人。E-mail：goldstar_8209@163.com

Lanthanide ions, especially Eu(Ⅲ) and Tb(Ⅲ), are excellent luminescent centers and the luminescent properties are influenced by ligands. Although the high and variable coordination numbers and flexible coordination environments of lanthanide ions may create complications in controlling reactions and thereby the final structures of products, the fascinating coordination chemistry and the rich structural properties along with numerous properties of lanthanide complexes have attracted increasing interest in their chemistry[8-10]. We are interested in the coordination chemistry of 4-chlorophenoxyacetic acid (4-Hcpoa), a flexible ligand with versatile binding and coordination modes, which has been proven to be useful in the construction of coordination polymers [11-14]. This is because the flexible 4-cpoa ligand will reduce the sterichindrance when coordinated to metal ions through carboxylate groups. However, so far, work on the construction of lanthanide complex based on 4-cpoa ligand and N-containing auxiliary ligands have not been reported. On the basis of above considerations, we chose 4-chlorophenoxyacetic acid (4-Hcpoa) and 1,10-phenanthroline (phen) as staring materials to construct the title dinuclear terbium complex, $[Tb_2(4\text{-Hcpoa})_5(phen)_2(NO_3)]$ (**1**), under hydro-thermal conditions. Structural characterization, luminescence and biological activities of **1** are reported here.

## 1 Experimental

### 1.1 Materials and measurements

All chemicals were commercially available and used as received without further purification. Elemental analyses for C, H, and N were carried out by using a Vario EL III Elemental Analyzer. Infrared spectra were recorded (4 000~400 $cm^{-1}$) as KBr disks on a Bruker 1600 FTIR spectrometer. Powder XRD investigations were carried out on a Bruker AXS D8-Advanced diffractometer at 40 kV and 40 mA with Cu $K\alpha$ ($\lambda$=0.154 06 nm) radiation. Luminescence spectra for crystal solid samples were recorded at room temperature on an Edinburgh FLS920 phosphorimeter. Thermogravimetry analyses (TGA) were performed on an automatic simultaneous thermal analyzer (DTG-60, Shimadzu) under a flow of $N_2$ at a heating rate of 10 ℃·$min^{-1}$ between ambient temperature and 800 ℃.

### 1.2 Synthesis of complex 1

A mixture of $Tb(NO_3)_3·6H_2O$ (0.226 g, 0.5 mmol), 4-Hcpoa (0.093 g, 0.5 mmol), phen (0.09 g, 0.5 mmol) and $H_2O$ (15 mL) was sealed in a 23 mL Teflon reactor and kept under autogenous pressure at 150 ℃ for 72 h. The mixture was cooled to room temperature at a rate of 5 ℃·$h^{-1}$ and colorless block crystals were obtained in a yield of 59% based on the Tb. Calcd. for $C_{64}H_{46}Cl_5N_5O_{18}Tb_2$ (%): C, 46.04; H, 2.76; N, 4.20. Found (%): C, 46.08; H, 2.70; N, 4.29. IR bands (KBr pellets, $cm^{-1}$): 3460 (s), 3018 (w), 1636 (m), 1599(s), 1520(m), 1481(m), 1428(m), 1384(s), 1316(m), 1167 (m), 1121(m), 1060(w), 1031(w), 856(s), 766(w), 740 (w), 726(w), 708(w), 602(w), 572(w), 528(w), 488(w).

### 1.3 Crystal structure determination

A colorless crystal with dimensions of 0.31 mm×0.25 mm×0.20 mm was selected for X-ray analyses. All diffraction data were collected on a Bruker Smart Apex II CCD diffractometer operating at 50 kV and 30 mA using a Mo $K\alpha$ radiation ($\lambda$=0.071 073 nm) at 296 (2) K by using a $\omega$ scan mode. In the range 1.91°≤$\theta$≤27.61°, a total of 20 476 reflections were collected, of which 7 432 were unique ($R_{int}$=0.025 1) and 6 339 observed ones ($I>2\sigma(I)$) were used in the succeeding structure calculations. Data collection and reduction were performed using the APEX II software[15]. Multi-scan absorption corrections were applied for all the data sets using the SADABS[15]. The structure was solved by direct methods and refined by full matrix least squares on $F^2$ using the SHELXTL program package[16]. All non-hydrogen atoms were treated anisotropically. The hydrogen atoms attached to C were added according to theoretical models. The final $R$=0.037 0 and $wR$=0.094 1 ($w=1/[\sigma^2(F_o^2)+(0.045\ 0P)^2+2.500\ 0P]$, where $P=(F_o^2+2F_c^2)/3$) for 6 339 observed reflections with $I>2\sigma(I)$. $S$=1.041, $(\Delta/\sigma)_{max}$=0.001, $(\Delta\rho)_{max}$=129.5 e·$nm^{-3}$ and $(\Delta\rho)_{min}$=−660 e·$nm^{-3}$. Crystal parameters and details of the data collection and refinement are given in Table 1. The selected bond lengths and bond angles are shown in Table 2. H-

bonding parameters for **1** are given in Table 3.

CCDC: 957432.

### 1.4 Biological activity test

The herbicidal activities of the ligand 4-Hcpoa and complex **1** were determined using *Brassica napus L. and Digitaria sanguinalis L.* as samples of dicotyledonous and monocotyledonous plants, respectively [17-18]. Solutions of the tested compounds were prepared by dissolving them in Dimethyl sulfoxide (100 μL) with the addition of Tween 20 (2 μL), and then diluting with distilled water. The germinated seeds were placed on two filter papers in a 9-cm Petri plate, to which 5 mL of tested solution was added in advance. Usually, 15 seeds were used on each plate. The plates were placed in a dark room and allowed to germinate for 72 h at 25 ℃. The lengths of 10 seed roots selected from each plate were measured and the means were calculated. Moreover, quizalofop-*p*-ethyl, a commercial aryloxy-phenoxy propionate herbicide and the emulsion which does not contain tested compounds were used as control and blank respectively. For all of the bioassay tests, each treatment was repeated three times. Then inhibitory rate was calculated relative to the blank. The bioassay results are shown in Table 4.

## 2 Results and discussion

### 2.1 IR spectra

The IR spectra of complex **1** shows broad bands in the 3 460 $cm^{-1}$, which may be assigned to the $\nu$(O-H) stretching vibrations of the water molecules (impurity). The moderate absorption band observed at 3 018 $cm^{-1}$ is attributed to the $\nu(C_{methylene}\text{-}H)$ vibration of 4-cpoa ligand. The features at 1 636 and 1 481, 1 428 $cm^{-1}$ are associated with the asymmetric (COO) and symmetric (COO) stretching vibrations. The $\Delta\nu(\nu_{as}(COO^-)-\nu_s(COO^-))$ values are 208 $cm^{-1}$ (greater than 200 $cm^{-1}$), and 155 $cm^{-1}$ (between 105 and 200 $cm^{-1}$) indicating the coordination of carboxylate with Tb(Ⅱ) in monodentate and bridging modes [19], which is well consistent with X-ray diffraction structural analysis.

### 2.2 Structure description

Single-crystal X-ray diffraction analysis reveals that compound **1** crystallizes in the $P\bar{1}$ space group and has a dinuclear structure. The Tb(Ⅲ) ions are bridged by two bidentate and two terdentate carboxylate groups to give centrosymmetric dimmers with Tb…Tb separation of 0.397 01(4) nm. The coordination environment for Tb(Ⅲ) ions of **1** is shown in Fig.1. Each Tb(Ⅲ) is coordinated by five O-donors (O2, O3, O5, $O5^i$, O6) of four different 4-cpoa ligands, two nitrogen atoms (N1 and N2) from one phen ligand, two oxygen atoms (O7 and O8 with 0.5 occupancy rate) from a half nitrate anion, one carboxylate oxygen atom (O10 with 0.5 occupancy rate) from a half 4-cpoa ligand (symmetry code: $^i$ 1−*x*, −*y*, 1−*z*). The Tb−O, Tb-N bond distances and O-Tb-O, O-Tb-N bond angles ranging from 0.232 7(3) to 0.281 8(7) nm and 51.24 (9)° to 152.2 (4)°, respectively, all of which are within the range of those observed for other Tb(Ⅲ) complexes with nitrogen and oxygen donors ligands[20-21]. The 4-cpoa ligands display three types of coordination. The first one acts as a conventional bidentate bridging ligand, bonding to Tb1 through O2 and $Tb1^i$ through O3 (Scheme 1a). The second one is chelated to Tb1 through O5, and O6, with O5 also linked to $Tb1^i$ (Scheme 1b). The third one is just unidentate coordinate to Tb1 through O10 (Scheme 1c). The structure has three distinct Tb-O distances involving 4-cpoa ligands depending on three coordination modes; average bond lengths of Tb-$O_{bridging}$, Tb-$O_{terdentate}$ and Tb-$O_{unidentate}$ are 0.234 5, 0.253 4 and 0.243 6 nm, respectively. This indicates that the order of ring strain is terdentate>unidentate>bridging. The separation of Tb…Tb (0.397 0 nm) in the dimer just exceeds the sum of the two ionic radii. The short separation may be attributed to the simultaneous appearance of four-membered and eight-membered rings between the two terbium atoms. The average Tb-N bond distance is 0.256 6 nm. Structures, including the complex **1** suggest strongly that N-bidentate heterocyclic amines as ligands have stronger coordination ability for lanthanide ions than N-unidentate ligands which are hard, and much less common. The centrosymmetric dinuclear molecules are connected into a 1D infinite chain through

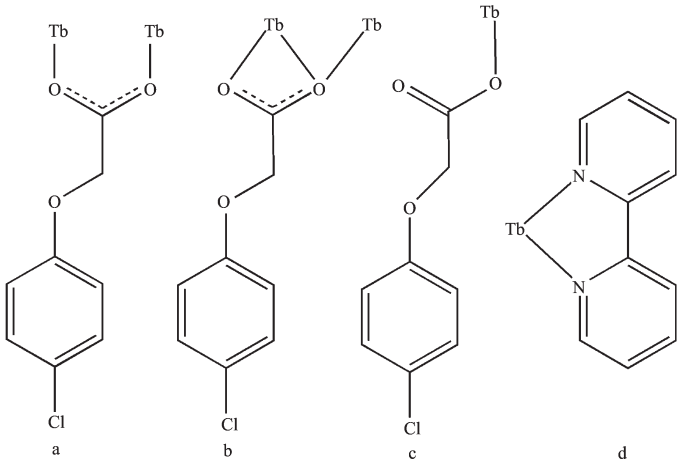


Scheme 1 Coordination modes of 4-Hcpoa and phen ligands in the structure of **1**

**Table 1 Crystal data and structure refinements of complex 1**

| | | | |
|---|---|---|---|
| Empirical formula | $C_{64}H_{46}Cl_5N_5O_{18}Tb_2$ | $\gamma$ / (°) | 83.166 0(10) |
| Formula weight | 1 668.15 | $V$ / nm$^3$ | 1.612 96(16) |
| Temperature / K | 296(2) | $Z$ | 1 |
| Size / mm | 0.31×0.25×0.20 | $\mu$ / mm$^{-1}$ | 2.457 |
| $\theta$ range for data collection / (°) | 1.91 to 27.61 | $D_c$ / (g·cm$^{-3}$) | 1.717 |
| Crystal system | Triclinic | $F$(000) | 824 |
| space group | $P\bar{1}$ | Reflections collected | 20 476 |
| $a$ / nm | 1.022 09(6) | Independent reflections($R_{int}$) | 7 432 (0.025 1) |
| $b$ / nm | 1.103 04(6) | Goodness of fit on $F^2$ | 1.020 |
| $c$ / nm | 1.513 38(9) | $R_1$, $wR_2$ ($I$>2$\sigma$($I$)) | 0.037 0, 0.094 1 |
| $\alpha$ / (°) | 75.725 0(10) | $R_1$, $wR_2$ (all data) | 0.046 2, 0.100 4 |
| $\beta$ / (°) | 77.948 0(10) | $(\Delta\rho)_{max}$, $(\Delta\rho)_{min}$ / (e·nm$^{-3}$) | 129.5, −660 |

**Table 2 Selected bond lengths (nm) and angles (°) for complex 1**

| | | | | | |
|---|---|---|---|---|---|
| Tb(1)-O(5)$^i$ | 0.232 7(3) | Tb(1)-O(2) | 0.234 2(3) | Tb(1)-O(3)$^i$ | 0.234 8(3) |
| Tb(1)-O(8) | 0.236 5(14) | Tb(1)-O(10) | 0.243 6(13) | Tb(1)-O(6) | 0.245 4(3) |
| Tb(1)-O(5) | 0.261 4(3) | Tb(1)-N(1) | 0.258 3(3) | Tb(1)-N(2) | 0.254 9(4) |
| | | | | | |
| O(5)$^i$-Tb(1)-O(2) | 75.25(11) | O(5)$^i$-Tb(1)-O(3)$^i$ | 76.49(11) | O(2)-Tb(1)-O(3)$^i$ | 135.29(11) |
| O(2)-Tb(1)-O(8) | 86.9(3) | O(3)$^i$-Tb(1)-O(8) | 124.8(3) | O(5)$^i$-Tb(1)-O(10)$^i$ | 80.4(4) |
| O(5)$^i$-Tb(1)-O(6) | 124.36(10) | O(2)-Tb(1)-O(6) | 87.63(12) | O(10)$^i$-Tb(1)-O(6) | 146.0(3) |
| O(5)$^i$Tb(1)-N(2) | 144.98(12) | O(5)$^i$-Tb(1)-N(1) | 144.71(12) | N(1)-Tb(1)-N(2) | 64.34(12) |

Symmetry codes: $^i$ 1−$x$, −$y$, 1−$z$

**Table 3 Hydrogen bonds of 1**

| D-H···A | $d$(D-H) / nm | $d$(H···A) / nm | $d$(D···A) / nm | ∠DHA / (°) |
|---|---|---|---|---|
| C(7)-H(7A)···O(9)$^{ii}$ | 0.097 | 0.258 | 0.351 09 | 161 |
| C(17)-H(17A)···O(2) | 0.093 | 0.233 | 0.297 77 | 126 |
| C(26)-H(26A)···O(3) | 0.093 | 0.240 | 0.302 94 | 125 |

Symmetry codes: $^{ii}$1+$x$, $y$, $z$

**Table 4　Herbicidal activities of 4-Hcpoa, complex 1 and quizalofop-*p*-ethyl**

| Compounds | Inhibitory rate / % | | | | | |
|---|---|---|---|---|---|---|
| | *Brassica napus L.* | | | *Echinochloa crusgalli L.* | | |
| | 100 mg·L$^{-1}$ | 50 mg·L$^{-1}$ | 10 mg·L$^{-1}$ | 100 mg·L$^{-1}$ | 50 mg·L$^{-1}$ | 10 mg·L$^{-1}$ |
| 4-Hcpoa | 33.1 | 29.2 | 14.6 | 92.7 | 86.6 | 41.6 |
| **1** | 40.9 | 32.4 | 18.8 | 98.2 | 92.4 | 48.3 |
| quizalofop-*p*-ethyl | 52.2 | 40.4 | 32.7 | 100 | 94.6 | 61.3 |

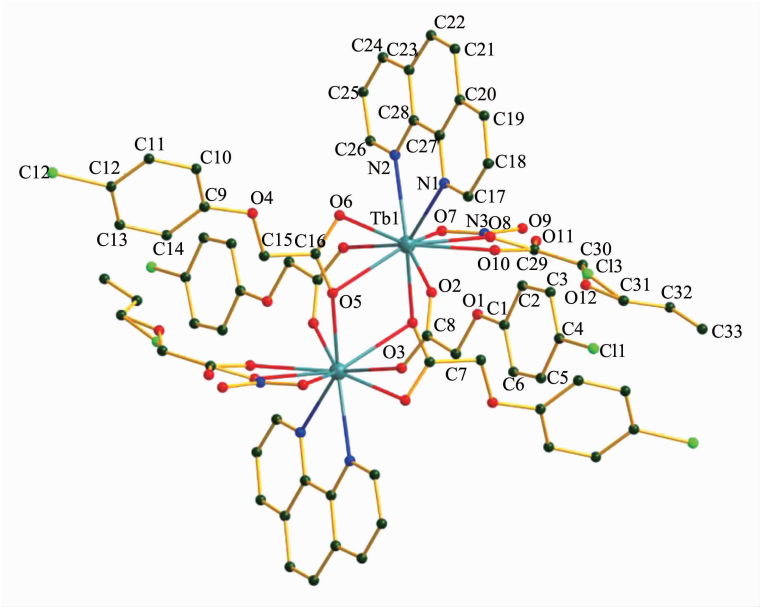


30% thermal ellipsoids, all H atoms are omitted for clarity

Fig.1　Diagram showing the coordination environment for Tb(Ⅲ) ions in **1**

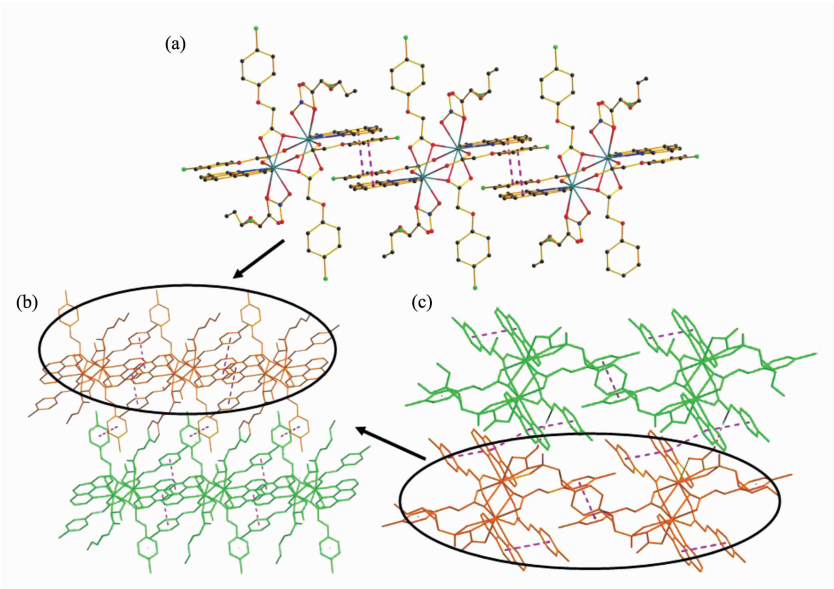


Fig.2　(a) View of 1D chain structure in **1** with $\pi\cdots\pi$ stacking interactions in dashed lines; (b) View of the 2D sheet in **1** with $\pi\cdots\pi$ stacking interactions stacking interactions in dashed lines; (c) View of the 3D supramolecular structure in **1** with C7-H7A···O9 hydrogen bonds and $\pi\cdots\pi$ stacking interactions in dashed lines

intermolecular $\pi\cdots\pi$ stacking interactions between benzene rings (Cg1 and Cg2) of 4-cpoa and phen ligands, with the centroid-to-centroid distance of 0.374 9(8) nm (Fig.2b). Adjacent chains are further connected into a 2D layered network through another $\pi\cdots\pi$ stacking interactions between benzene rings (Cg3) of 4-cpoa ligands, with the centroid-to-centroid distance of 0.369 6 (7) nm (Fig.2a). These layers are finally linked via C7-H7A···O9 hydrogen bonds and $\pi\cdots\pi$ stacking interactions between benzene rings (Cg2) of phen ligands into a three-dimensional supramolecular structure (Fig.2c) (Cg1, Cg2 and Cg3 are the centroid of the C1-C6 ring, C20-C23/C27/C28 ring, and C9-C14 ring, respectively). Moreover, intramolecular C-H ··· O hydrogen bonds are also observed (Table 3).

### 2.3 Thermal analysis

The thermogravimetric analyses (TGA) of compound **1** were performed in a $N_2$ atmosphere when the sample was heated to 800 ℃ at a constant rate of 10 ℃·min$^{-1}$. The TG and DTA curves are depicted in Fig.3, which shows that compound **1** has good thermal stability as no strictly clean weight loss step occurs below 250 ℃. The weight-loss step occurred above 250 ℃ which corresponds to the decomposition of framework structure. Finally, **1** was completely degraded into $Tb_2O_3$ with total loss of 78.21% (Calcd. 78.06%).

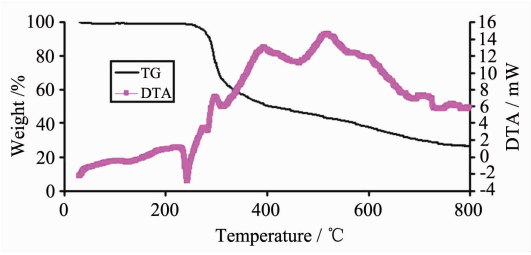


Fig.3 Thermogravimetric curves (DTA and TG) for complex **1**

### 2.4 Powder X-ray Diffraction Analysis

Samples of complex **1** were measured by X-ray powder diffraction at room temperature, as shown in Fig.4.

Although the experimental patterns have a few un-indexed diffraction lines and some are lightly broadened in comparison with those simulated from the single-crystal data using Mercury, it still can be well considered that the bulk synthesized materials and the crystals used for diffraction are homogeneous.

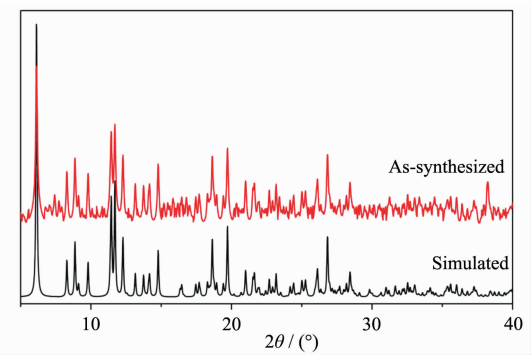


Fig.4 PXRD patterns in complex **1**

### 2.5 Luminescent properties

The metal-organic hybrid coordination polymers with lanthanide metal centers have been widely investigated for their fluorescence properties. The lanthanides only exhibit weak emissions under direct excitated due to their low molar absorptivity. Lanthanide-centered emission can be sensitized by coordinating to the organic ligands with $\pi$-systems, which can efficiently absorb and transfer the energy. Solid-state excitation and emission luminescence spectra of **1** at room temperature are shown in Fig.5. There are four main emission peaks in the emission spectrum of **1** with the excitation wavelength at 321 nm, ascribed to the characteristic emission of Tb (Ⅲ), and corresponding to electronic transitions from the emitting level $^5D_4$ to the ground multiplet $^7F_n$ ($n$ = 6 →3) [22]. The most intense emission at 544 nm corresponds to $^5D_4\rightarrow{}^7F_5$ transition. The second-most

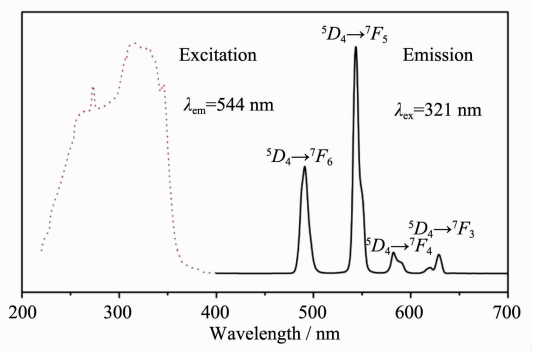


Fig.5 Solid-state excitation and emission spectra of complex **1** at room temperature

intense emission at 492 nm corresponds to $^5D_4 \rightarrow {}^7F_6$ transition. The bands at 580 and 630 nm correspond to the $^5D_4 \rightarrow {}^7F_4$ and $^5D_4 \rightarrow {}^7F_3$ transitions of the Tb(Ⅲ) ion, respectively. The luminescent lifetime of solid complex **1** using an Edinburgh FLS920 phosphorimeter with 450 W xenon lamp as excitation source show lifetime for complex **1** of 0.920 ms at 544 nm (Fig.6).

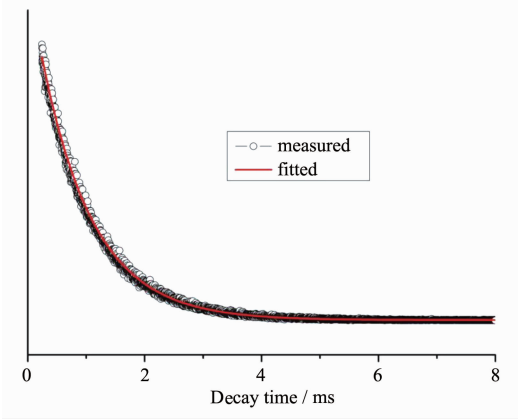


Fig.6　Luminescent lifetime for complex **1** in solid state at room temperature

### 2.6　Biological activity

Indole-3-acetic acid (IAA), 1-naphthalene acetic acid (1-NAA), 2-methyl-4-chlorophenoxyacetic acid (MCPA) and 2,4-dichlorophenoxyacetic acid (2,4-D) are well known as herbicides for weed control[23]. 4-chlorophenoxyacetate and its lanthanide complex were chosen as herbicides according to the following considerations: (1) 4-Hcpoa belongs to aromatic acetic acid, which maybe exhibit good herbicidal activities; (2) it has been found that the biological activities of ligand maybe activated by metallic ions[24]. Herein, the herbicidal activities of ligand 4-Hcpoa and complex **1** were investigated and shown in Table 4. In all tested compounds, the rates of inhibition of *Brassica napus L.* root growth are 33.1%~40.9%, 29.2%~32.4% and 14.6%~18.8% at concentrations of 100, 50 and 10 mg·L$^{-1}$, respectively, which means that the 4-Hcpoa and complex **1** display low herbicidal activities against this plant. However, the rates of inhibition of *Echinochloa crusgalli L.* Root growth are high (92.7%~98.2%) at a concentration of 100 mg·L$^{-1}$, 86.6%~92.4% at 50 mg·L$^{-1}$, and 41.6%~48.3% at 10 mg·L$^{-1}$. The results reveal that three samples exhibit excellent herbicidal activities against this kind of weed at 100 mg·L$^{-1}$ and 50 mg·L$^{-1}$, but their activities are not satisfactory at a lower concentration (10 mg·L$^{-1}$). Moreover, we found that the complexes shows superior effective than ligand 4-Hcpoa. It is possible that the ligand 4-Hcpoa may be activated by the $Tb^{3+}$ ion[24].

## 3　Conclusion

In conclusion, a new dinuclear terbimu (Ⅲ) complex based on 4-Hcpoa and phen ligands, $[Tb_2(4\text{-Hcpoa})_5(phen)_2(NO_3)]_n$ has been hydrothermal synthesized and structurally characterized. Complex **1** emits the intensely green luminescence with the fluorescence lifetime of 0.920 ms (544 nm) in the solid state at room temperature. Preliminary bioassay indicates that ligand 4-Hcpoa and complex **1** exhibit high herbicidal activities against monocotyledonous plant such as *Echinochloa crusgalli L.* at concentrations of 100 mg·L$^{-1}$ and 50 mg·L$^{-1}$.

**References**:

[1] Ma D, Lu K, Guo H, et al. *J. Mol. Struct.*, **2012**,**1021**:179-186
[2] Galdwell J P, Henderson W, Kim N D. *J. Forensic Sci.*, **2001**,**46**:1332-1341
[3] Tsukube H, Juanes S. *Chem. Rev.*, **2002**,**102**:2389-2403
[4] Lin S, Feuerstein R J, Mickelson A. *J. Appl. Phys.*, **1996**,**79**:2868-2874
[5] Kido J, Okamoto Y. *Chem. Rev.*, **2002**,**102**:2357-2368
[6] Ma D, Wang W, Li Y, et al. *CrystEngComm*, **2010**,**12**:4372-4377
[7] Kapoor P, Singh R V, Fahmi N. *J. Coord. Chem.*, **2012**,**65**:262-277
[8] Liang Y C, Cao R, Su W P, et al. *Angew. Chem. Int. Ed.*, **2000**,**39**:3304-3307
[9] Jana A, Majumder S, Carrella L, et al. *Inorg. Chem.*, **2010**,**49**:9012-9025
[10]Koner R, Lee G H, Wang Y, et al. *Eur. J. Inorg. Chem.*, **2005**,1500-1505
[11]Wang Z, Liu D S, Zhang H H, et al. *J. Coord. Chem.*, **2008**, **61**:419-425
[12]Sun R Q, Zhang H H, Cao Y N, et al. *Chinese J. Struct. Chem.*, **2006**,**25**:844-848
[13]Sun Y, Wang Z, Zhang H, et al. *Inorg. Chim. Acta*, **2007**,

**360**:2565-2572

[14]Shi S M, Chen Z F, Liu Y C, et al. *J. Coord. Chem.*, **2008**, **61**:2757-2734

[15]Bruker. *APEXII Software*, *Version* 6.3.1, Bruker AXS Inc, Madison, Wisconsin, USA, **2004**.

[16]Sheldrick G M. *Acta Cryst.*, **2008**,A64:112-122

[17]MU Li-Yi(慕立义). *Research Method of Plant Chemical Protection*(植物化学保护研究方法). Beijing: China Agriculture Press, **1994**:90

[18]Wang B L, Duggleby R G, Li Z M, et al. *Pest Manag. Sci.*, **2005**,**61**:407-412

[19]Zheng Y, Xu D M, Liu S X. *Inorg. Chim. Acta*, **1999**,**294**: 163-169

[20]Barja B, Aramendia P, Baggio R, et al. *Inorg. Chim. Acta*, **2003**,**355**:183-190

[21]Fu A Y, Wu Y P, Wang F M, et al. *J. Coord. Chem.*, **2010**, **63**:3724-3733

[22]Zhao B, Chen X Y, Cheng P, et al. *J. Am. Chem. Soc.*, **2004**,**126**:15394-15395

[23]Grossmann K. *J. Plant Growth Regul.*, **2003**,**22**:109-122

[24]Offiong O E, Nfor E, Ayi A A, et al. *Transition Met. Chem.*, **2000**,**25**:369-373